PROCEEDINGS A

rspa.royalsocietypublishing.org

Research

Article submitted to journal

Subject Areas:
fluid mechanics, physical chemistry, mathematical modelling

Keywords:
Foam rheology, foam films, surfactant transport, Gibbs elasticity, meniscus, mathematical modelling

Author for correspondence:
P. Grassia
e-mail: paul.grassia@strath.ac.uk

THE ROYAL SOCIETY
PUBLISHING

Analysis of a model for surfactant transport around a foam meniscus

P. Grassia[1]

[1] Department of Chemical & Process Engineering, University of Strathclyde, James Weir Building, 75 Montrose St, Glasgow G1 1XJ, UK.

A model developed by [1] is considered for film-to-film surfactant transport around a meniscus within a foam, with the transport rate dependent upon film-to-film tension difference. The model is applied to the case of a five-film device, in which motors are used to compress two peripheral films on one side of a central film and to stretch another two peripheral films on the central film's other side. Moreover it is considered that large amounts of compression or stretch are imposed on peripheral films, and also that compression or stretch might be imposed at high velocities (relative to a characteristic velocity associated with physicochemical properties of the foam films themselves). The actual strain that results on elements within each film might differ from the imposed strain, with the instantaneous film length coupled to the actual strain determining the amount of surfactant currently on each film (and hence also the amount of surfactant that has transferred either from or onto films). Quite distinct surfactant transport behaviour is predicted for the stretched film compared to the compressed one. In particular when a film is stretched sufficiently at high enough velocity, surfactant flux onto it is predicted to become extremely "plastic", increasing significantly.

1. Introduction

As well being familiar in everyday life [2–5] and useful in myriad industrial processes [6–12], foams have long held a fascination for physicists. The reason for this fascination is well documented [13,14]: foams films reduce their surface energy by reducing their surface area, meaning that films are minimal surfaces subject to the constraint that bubbles fill certain volumes [15–18].

Similar notions (i.e. constrained minimization of area)

can also be used to study foam rheology [19]. Starting from a relaxed con guration, the boundaries of a foam can be subject to deformation, and the foam needs to nd new minimal surface states subject to those additional constraints on the boundary [20–24]. Generally this involves higher energy cost than before. However for suf cient deformation, it may be the case that certain lms shrink away to zero size, so bubbles formerly in contact will detach from one another and other bubbles will come into contact in their place, forming new lms [22]. This process, known as a topological transformation [13,25,26], helps the surface energy to relax thereby allowing the foam to yield plastically [20,23,24], and subsequently to approach a new mechanical equilibrium.

Despite the very valuable insights into foam physics and/or foam rheology that can thereby be gained, the body of work described above neglects one important aspect of foams, namely physical chemistry. In fact, aqueous foams are typically produced with the aid of chemical additives i.e. surfactants [27]. As soon as one starts deforming the foam lms, necessarily surfactant starts moving around also [28–30]: physicochemical effects associated with surfactant transport thereby couple with foam ow and foam lm deformation [31–38].

The behaviour of the foam then relies on the interplay between many different time scales [31, 32,39–45] involving at the very least a characteristic time scale for imposed deformation, a characteristic time scale for mechanical relaxation of the foam, and a characteristic time scale for physicochemical relaxation of the foam, i.e. a time scale associated with surfactant transport. If there happen to be multiple mechanisms for surfactant transport [46], there may of course be more than one physicochemical time scale.

In many ways these physicochemical aspects of foams are more dif cult to deal with than the physical (i.e. minimal surface) aspects are: foam lm geometry can be easily observed directly, but individual surfactant molecules cannot. Hence information about surfactant behaviour must be inferred from other measurements [47,48], often utilising techniques that determine surface tension [49,50]. What is known is that stretching the lm depletes the amount of surfactant on the surface, leading to an increase in lm tension [51], a phenomenon known as Gibbs elasticity [52].

Although the in uence of surfactants upon foam lm surfaces is thereby well documented, very often physical chemistry studies like these have focussed upon geometrically simple systems, either the interface of a single droplet or a single bubble or indeed just a single lm [28,47,53–55]. Whilst studies like these do give valuable insights into surfactant transport within and along individual lm surfaces, they still fall short of understanding how surfactant is transported within a foam as a whole. Indeed one mechanism that studies on individual lms cannot capture, but which must be relevant in foams (albeit neglected in at least one previous study [38] owing to lack of an adequate model) is surfactant transport from a foam lm to its neighbouring lms [56].

This mechanism certainly will be relevant in the aforementioned topological transformation process [13,20,23]. Films that shrink and then disappear on the approach to the topological transformation presumably must transport surfactant over to neighbours. Meanwhile new lms that are created during the topological transformation start out with small size, but are necessarily stretched as the foam then relaxes mechanically. Stretching in isolation would cause the lm to deplete in surfactant, but this can be compensated if it receives surfactant from its neighbours. Speci cally this requires a surfactant ux around the menisci joining any neighbouring lms to the newly formed lm of interest.

There have been various hypotheses [57–59] for what the surfactant ux should be around such menisci, all based on the idea that Marangoni effects drag material from low tension (high surfactant concentration on the surface) to high tension (low surfactant concentration on the surface). Often though hypotheses like these have been largely empirical. Nevertheless a recent study [1] (see also [60] for a brief commentary thereon) including both a rigorous uid mechanical analysis and an experimental study (using the same apparatus already introduced in [56]) has now placed these sorts of hypotheses on a rmer basis.

The uid mechanical analysis of [1] identi ed clearly the main challenge with determining lm-to- lm surfactant uxes, namely so called geometrical frustration. At a meniscus, also known in the context of foams as a Plateau border [13], three lms meet. As a result, a lm that is passing surfactant to or receiving surfactant from one of its neighbours only communicates with that neighbour on one side. The other side of the lm in question contacts a different neighbour, possibly in a very different state from the neighbour on the original side, and hence possibly involving a different amount of surfactant transport. Close to a meniscus, a model therefore ought somehow to account for different sides of an individual lm having different amounts of surfactant (a point we will return to in section 2(b)iii), even though further away from the meniscus, such differences are less signi cant.

Meanwhile, the experimental system studied by [1] whilst not quite the same as what happens during a topological transformation, nor anywhere near as complex as a general foam, is nevertheless far more complex than just a single lm would be. Speci cally it was a ve- lm device (see e.g. Figure 1) with a central lm connecting to four peripheral lms, two on each side of the central lm. The system could be driven by motors, such that the two peripheral lms on one side of the central lm are compressed, and the two peripheral lms on the other side are stretched. Surfactant could then be transported from the compressed lm to the central lm and from the central lm to the stretched lm (more detail on this is given in section 2(a)). However such transport is affected, as already alluded to above, by geometrical frustration (see Figure 1(c)).

The system permitted a constitutive relation between lm-to- lm tension difference and surfactant ux around the meniscus [1] to be proposed and tested (detailed discussion of the relation itself is deferred to section 2(b)). Using this constitutive relation, equations were proposed (again detailed discussion is given later, namely in section 2(c)) governing the evolution of how much surfactant nds its way from lm to lm, both while motors are switched on and after they are switched off. However these equations were only solved by [1] in a limited scenario in which just small amounts of compression or stretch were imposed (i.e. in a limit of small imposed strains), and hence just small amounts of surfactant were transferred. Solutions for the surfactant transport involving simple exponential decays then resulted.

The constitutive relation developed by [1] was not itself restricted to small imposed strains. It is merely the case that when [1] developed a model for the ve- lm device as a whole (the constitutive relation being just one of the ingredients of that model), solutions were only tackled in the limit of small imposed compression or stretch. The purpose of the present work is to return to the model of [1] but imposing larger amounts of compression or stretch, beyond the regime of validity of the aforementioned simple exponential solutions. As we will see, surfactant manages to escape from the compressed lm, without accumulating excessively, even if the compression is very strong. Meanwhile for the stretched lm, if a signi cant amount of stretch is imposed at a suf cient rate, the constitutive relation allows surfactant to be transported rather more quickly onto the lm. Even though the present work treats only the ve- lm device of [1] and not a general foam, gaining insights into behaviours of lms subject to large amounts of compression or stretch is deemed of interest: the aforementioned topological transformations occurring in a general foam do of course involve lms subject to large amounts of compression or stretch.

The rest of this work is laid out as follows. In section 2 we review the constitutive relation of [1] and surfactant transport equations that it implies. In section 3 we explain how to solve these equations even in a scenario of large imposed strains. Results obtained from these solutions are presented/discussed in section 4. Conclusions are given section 5. Some technical details of both the model and the solution procedure are relegated to appendices (in supplementary material).

2. Model and governing equations

In this section we review the model and governing equations proposed by [1]. The presentation is given within three subsections. The rst of these (section 2(a)) looks at surfactant transport around a meniscus. Then section 2(b) considers how to relate that transport to lm-to- lm tension differences. After that section 2(c) then shows how to incorporate strains that are imposed on

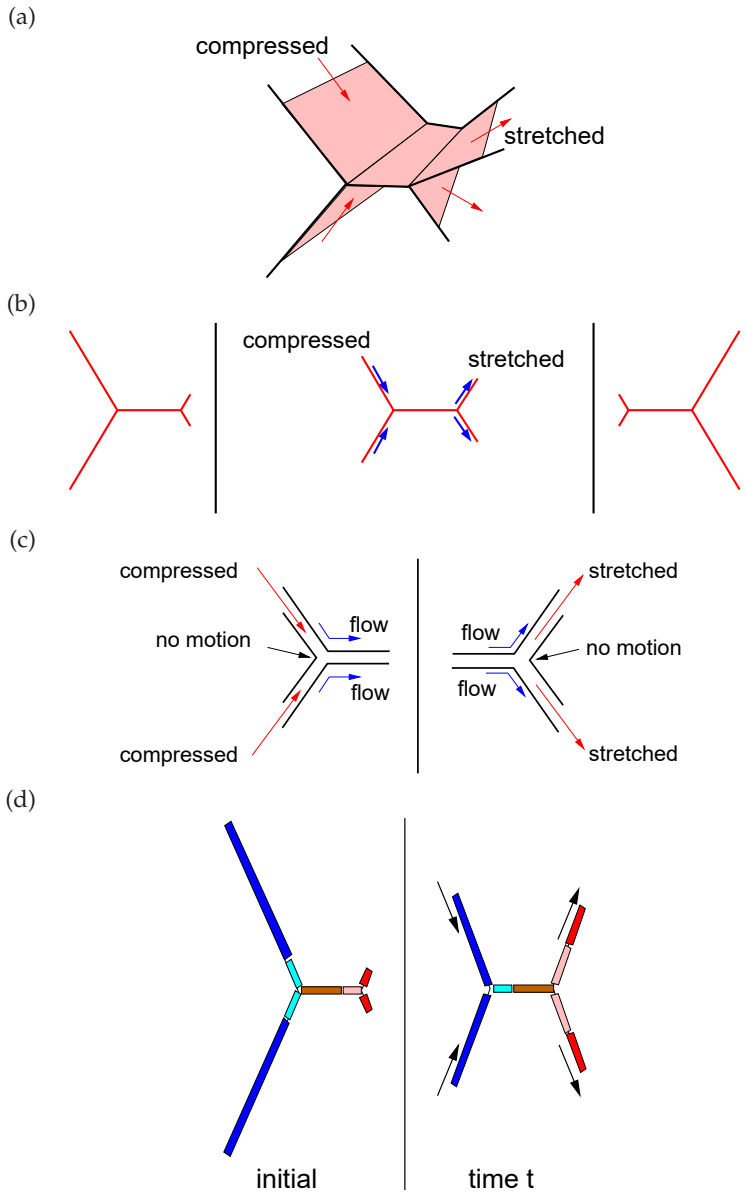

Figure 1. Sketch of the ve- lm device. (a) 3-D view. (b) 2-D view showing initial state (left), stretching or compression by a motor (middle) and the state after motor motion is complete (right). (c) Zoomed view close to the meniscus for the compressed lm (left) and stretched lm (right). This shows geometrical frustration, i.e. close to the meniscus, it is not possible to have the same ow on both sides of every lm. (d) Lagrangian lm elements (colour coded) which are used to determine the amount of surfactant on each lm in the ve- lm device. It is rst identi ed (via the colour coding) which Lagrangian elements are on given lm at a given time t subject to compression or stretch (right) and then the length which those elements had initially, prior to any compression or stretching, is determined (left), from which the amount of surfactant is then known.

various lms by the action of motors. In particular, section 2(c) is formulated in a fashion that lends itself to dealing with large strains, involving a slightly different way of expressing the model than the formulation that [1] used. The formulations are nonetheless equivalent. Readers already familiar the work of [1] may wish to skip directly to section 2(c) and in particular equation (2.13) which expresses the model in a compact and elegant form.

(a) Surfactant transport around a foam meniscus

Considering the compressed lm in the rst instance, the amount of surfactant on the lm at any instant is represented by a quantity $\mathcal{L}_0$, which is de ned as follows. Accounting just for the lm elements that are currently on the compressed lm, not those that have already been transferred from the compressed lm to the central lm (see Figure 1(d) for an illustration), the value of $\mathcal{L}_0$ represents the length that these elements had before the structure was set into motion.

If we happen to know the instantaneous velocity U at the meniscus (in the direction from the compressed lm to the central lm), then we can determine how $\mathcal{L}_0$ evolves with time t. Speci cally it was proposed [1]

$$\mathrm{d}\mathcal{L}_0 \ \mathrm{d}t = \ U \ \ (1 + \ \ ) \tag{2.1}$$

where is the instantaneous strain in the compressed lm upstream of the meniscus. Here is negative ($1 <$ < 0), i.e. the lm is compressed. Thus $\mathrm{d}\mathcal{L}_0$ $\mathrm{d}t$ exceeds the value of U , which follows because, for a given velocity at the meniscus, a greater surfactant ux results if surfactant has been concentrated due to the lm elements having been already compressed.

An analogous relationship applies for the stretched lm

$$\mathrm{d}\mathcal{L}_0^+ \ \mathrm{d}t = U^+ \ (1 + \ ^+) \tag{2.2}$$

which we interpret as follows. The value of $\mathcal{L}_0^+$ refers to the original length (before the structure was set into motion) of all the lm elements that are currently on the stretched lm. Not all these elements will have originated on the stretched lm however. Instead some of them might have arrived from the central lm (again see Figure 1(d) for an illustration). Moreover the instantaneous velocity U^+ is de ned at the meniscus in the sense from the central lm to the stretched lm. Also the strain $^+$ in the stretched lm downstream of the meniscus is positive. A consequence is that $\mathrm{d}\mathcal{L}_0^+$ $\mathrm{d}t$ is smaller than U^+. For a given velocity at the meniscus, surfactant ux is less if surfactant is depleted due to having stretched lm elements.

To complete the model of [1], it is necessary to provide constitutive relations to determine the velocities U and U^+. These are discussed in the next section.

(b) Constitutive relations for velocities at the menisci

Velocities U and U^+ at the menisci were taken by [1] to be functions of the differences in tensions between adjacent lms (with lm tensions being twice the surface tension here, as lms have two sides). Accordingly differences in lm tensions are discussed in section 2(b)i. The amounts of surfactant ux that these tension differences then manage to produce are discussed in section 2(b)ii (compressed case) and section 2(b)iii (stretched case). As we will see, the stretched case turns out to be somewhat more complicated than the compressed one.

(i) Differences in lm tensions

The tension differences required are respectively between the central lm and the compressed lm, and between the stretched lm and the central lm, and will be denoted $_c$ and $_{c+}$. Both of these tension differences (central to compressed, and stretched to central) are expected to be positive because the compressed lm should have the lowest tension of all, the central lm should have an intermediate tension and the stretched lm should have the highest tension. It was argued by [1] that on symmetry grounds the central lm does not undergo either stretching

or compression to any signi cant degree, and hence is assumed to have a tension that is always close to an equilibrium tension $_e$. It follows then that

$$_c = _e \tag{2.3}$$

$$_{c+} = _e{}^{+} \tag{2.4}$$

where $_e$ is the deviation from equilibrium tension in either the compressed or stretched lm. This should be negative in the compressed lm, but positive in the stretched lm, i.e. it should have the same sign as the lm strain . A Gibbs elasticity model was then invoked by [1] relating the lm tension deviation from equilibrium to the lm strain. This gave

$$_e = 2E \quad (1 + \quad) \tag{2.5}$$

where the factor 2 recalls that lms have two sides, and where E is the Gibbs elasticity parameter. Although the value of E could in principle itself vary with strain, it was treated by [1] as being constant. As we will see (in section 2(c)), this turns out to be convenient mathematically as it makes the system somewhat easier to solve. Physically what equation (2.5) means is as follows: although $_e$ is clearly nonlinear in , if it is plotted instead against the surfactant concentration on the lms, a straight line plot then results [1] as surfactant concentration turns out to scale inversely with $1 +$, and also $_e$ $2E$ $2E$ $(1 +$).

Moreover in the experimental work carried out by [1], lm strains could be determined by measuring lm thickness (using interferometric techniques): the more lm elements are stretched, the thinner they become. Meanwhile lm tension differences could be determined experimentally by measuring the angles at which lms meet at a meniscus, these angles being found in turn via the displacement of the meniscus relative to its equilibrium position: lms meeting at unequal angles imply unequal tension. Since lm strains and lm tensions can thereby be determined via the above mentioned measurements, and the values thus obtained compared with equation (2.5), experimental support is available for using equation (2.5) with E treated as constant. As alluded to earlier, this makes the system easier to solve.

To summarise we reiterate the signs of various terms. Recalling that < 0 in the compressed lm, it follows from equation (2.5) that $_e < 0$, i.e. tension is less than equilibrium as we expect. On the other hand, for the stretched lm $^{+} > 0$, so that $_e{}^{+} > 0$, i.e. tension exceeds equilibrium. Via equations (2.3)–(2.4) it then follows that $_c$ and $_{c+}$ have the correct signs (both positive) to drive surfactant ux around the menisci in the expected directions (from compressed lm to central lm and from central lm to stretched lm), and so we can proceed to consider constitutive relations expressed in terms of these tension differences.

(ii) Constitutive relation for compressed lm

In the rst instance, the compressed lm is considered. By examining numerous sets of data, it was found [1] that there was a proportionality relationship between U and $_c$ or equivalently a proportionality relationship between U and a dimensionless quantity $_c$ $(2E)$, remembering here that E is treated as being constant. The coef cient of proportionality, which has units of velocity, was denoted U . This coef cient can be thought of as a property of the foam lm, but is independent of how quickly the lm is compressed. A formula was also proposed [1] for how U should depend on various physicochemical properties of the lm (see appendix A), and by using it, different data sets could be collapsed together well. In the case of the compressed lm, proportionality between U and $_c$ $(2E)$ could continue to apply even for $_c$ $(2E)$ values well in excess of unity, i.e. U well in excess of U . The only restriction was an obvious physical one, i.e. the central lm remains by assumption at equilibrium tension whilst the compressed lm can have a much smaller tension, so that $_c$ can never exceed the equilibrium tension (denoted $_e$) but may well exceed $2E$.

Given that tension difference and strain are related via equation (2.5), it turns out to be convenient to rewrite U in terms of strain, remembering also here that is a negative quantity.

Via equation (2.3) and equation (2.5) it follows

$$U \quad = \quad U \qquad (1 + \quad) \tag{2.6}$$

and thence (via equation (2.1))

$$\mathrm{d}\mathcal{L}_0 \quad \mathrm{d}t = U \qquad (1 + \quad)^2 \tag{2.7}$$

We will revisit this equation later on (see equation (2.12)). Note that [1] did not formally derive this equation in the speci c form shown here, but it turns out to be very useful in the large strain limit that we will consider later on.

(iii) Constitutive relation for stretched lm

Now we return to the stretched lm. Examining numerous sets of data, a proportionality relationship was again found [1] between U^+ and $_{c+}$ $(2E)$, with the proportionality coef cient being the same U as before. This led via analogous arguments using now equation (2.4) and equation (2.5) to

$$U^+ = U \quad ^+ (1 + \quad ^+) \tag{2.8}$$

and thence (via equation (2.2))

$$\mathrm{d}\mathcal{L}_0^+ \quad \mathrm{d}t = U \quad ^+ (1 + \quad ^+)^2 \tag{2.9}$$

which, although again being an equation not formally derived by [1], will be useful later on.

It was argued by [1] that the relationship between meniscus velocity and tension difference in the stretched case is more constrained than before. The value of $_{c+}$ $(2E)$ (which via equation (2.4) is equal to $_e{}^+$ $(2E)$) was not allowed to exceed 1 2, or equivalently (via equation (2.5)), $^+$ was not allowed to exceed unity. If $^+$ ever did attain the value unity, then U^+ would take whatever value was needed, even a value well in excess of the prediction U 2 now obtained from equation (2.8), in order to prevent $^+$ from exceeding unity and thereby in turn preventing $_e{}^+$ $(2E)$) from exceeding 1 2. Thus the strain $^+ = 1$ corresponds to the ow U^+ at the meniscus suddenly becoming very plastic, which then helps to transport surfactant onto the stretched lm.

At rst sight it seems surprising that the system becomes plastic when $_e{}^+$ $(2E)$ reaches the value 1 2. After all, according to equation (2.5), the value $_e{}^+$ $(2E)$ could reach up to unity for an even more strongly stretched lm ($^+$ 1). However the explanation why $_e{}^+$ $(2E)$ is capped at 1 2 has been provided by [1] as being due to geometrical frustration (already alluded to in the introduction). Even though conventionally we think of the two sides of a lm as being the same in terms of their surface tension, so the lm tension is exactly twice the surface tension on either side, and this is indeed true over most of the lm length, suf ciently close to the meniscus this rule does not apply (see Figure 1(c)). Locally ow might be different on different sides of a lm, and that impacts surface tension. Film tension remains the sum of the surface tensions either side of the lm, albeit the tensions either side need not be the same.

For instance in the ve- lm device (see Figure 1 and in particular Figure 1(c)), one side of the stretched lm communicates with the central lm (and can receive a supply of surfactant from it), while the other side is in contact only with another stretched lm. This latter side is then the one which can deplete in surfactant but, as a result of even very strong depletion, at most its individual surface tension can increase by an amount E relative to equilibrium, at least in the model of [1] assuming a constant Gibbs elasticity parameter. This then also sets the cap on the amount that lm tension can increase above equilibrium. Moving slightly away from the meniscus, it was explained by [1] that the two surfaces of the lm adjust (whilst keeping the same overall lm tension) such that the surface tension on each side (and likewise the surface strain on each side) come into balance, and that then is the strain used to determine the lm tension in equation (2.5). The important point as far as the present work is concerned is then as follows. As long as the correct cap on lm tension and hence on lm strain is applied, the constitutive

equation determining the lm-to- lm surfactant ux can be utilised, even without having full details of the geometrical frustration induced behaviour at the meniscus itself.

(c) Model incorporating imposed strains in ve- lm device

Using the constitutive relations described above that govern U and U^+, a model could be proposed [1] for the behaviour of the ve- lm device. The model developed (see equation (2.13) below) is a "lumped parameter" model. What this means is that it treats the strain in the compressed or stretched lms as being spatially uniform (at least away from the meniscus) but different from the strain in the central lm, which (as already alluded to in section 2(b)) by assumption vanishes. We comment that in what follows, the equations are presented slightly differently from the way in which [1] chose to present them: speci cally we work in terms of lm strains rather than lm tensions. This slightly different (albeit mathematically equivalent) presentation helps to elucidate the mathematical structure of the model, which then makes it clearer how to solve it (see section 3), particularly when large strains are involved as we consider here. As mentioned already, even though the constitutive relation of [1] can cope with large strains, the lumped parameter model for the ve- lm device itself was only tackled by [1] in the small strain limit.

The model begins from the de nition of the "lumped" strain on the lms

$$\mathcal{L} \quad = (1 + \quad)\mathcal{L}_0 \tag{2.10}$$

where $\mathcal{L}$ is the instantaneous length of either the compressed or stretched lm, and and $\mathcal{L}_0$ are as given previously. We differentiate this with respect to time t to obtain

$$\mathrm{d}\mathcal{L} \quad \mathrm{d}t = (1 + \quad)\mathrm{d}\mathcal{L}_0 \quad \mathrm{d}t + \mathcal{L}_0 \ \mathrm{d} \quad \mathrm{d}t \tag{2.11}$$

We now eliminate terms in $\mathcal{L}_0$ and $\mathrm{d}\mathcal{L}_0 \quad \mathrm{d}t$ from the right hand side of equation (2.11). Using equation (2.10), it follows $\mathcal{L}_0 = \mathcal{L} \quad (1 + \quad)$. Meanwhile equation (2.7) and (2.9) give us the expression for $\mathrm{d}\mathcal{L}_0 \quad \mathrm{d}t$ which is

$$\mathrm{d}\mathcal{L}_0 \quad \mathrm{d}t = \quad U \quad (1 + \quad) = U \qquad (1 + \quad)^2 \tag{2.12}$$

noting however that in the case of stretching in particular, the second equality in equation (2.12) is only valid when $^+ < 1$. If instead $^+$ reaches the value unity and stays xed there, equation (2.10) gives $\mathrm{d}\mathcal{L}_0^+ \quad \mathrm{d}t = (1 \ \ 2)\mathrm{d}\mathcal{L}^+ \quad \mathrm{d}t$. In the case when $^+ = 1$, equation (2.2) gives $\mathrm{d}\mathcal{L}_0^+ \quad \mathrm{d}t = U^+ \ \ 2$ and hence it follows $U^+ = \mathrm{d}\mathcal{L}^+ \quad \mathrm{d}t$. This relation holds instead of U^+ satisfying equation (2.8), which for $^+ = 1$ would give instead a value of $U \quad 2$. Thus as long as $\mathrm{d}\mathcal{L}^+ \quad \mathrm{d}t$ exceeds $U \quad 2$, a jump in U^+ must occur once $^+ = 1$. The surfactant transport rate $\mathrm{d}\mathcal{L}_0^+ \quad \mathrm{d}t$ likewise jumps from $U \quad 4$ to the aforementioned value $(1 \ \ 2)\mathrm{d}\mathcal{L}^+ \quad \mathrm{d}t$ once $^+ = 1$.

In the rst instance though, we consider $^+ < 1$. Upon multiplying equation (2.11) through by $1 + \quad$, and substituting from equation (2.12), this leads to

$$(1 + \quad)\mathrm{d}\mathcal{L} \quad \mathrm{d}t = U \qquad + \mathcal{L} \quad \mathrm{d} \qquad \mathrm{d}t \tag{2.13}$$

Now in the ve- lm device, $\mathcal{L}$ is a known function of t. Speci cally if $\mathcal{L}_i$ is the initial lm length (which generally is not the same for the compressed and stretched lms, see e.g. Figure 1(b)), and V is the velocity at which the motor compresses or stretches the lms, we have

$$\mathcal{L} \quad = \mathcal{L}_i \qquad V t \tag{2.14}$$

from which it also follows $\mathrm{d}\mathcal{L} \quad \mathrm{d}t = \quad V$. Note that the strain imposed on the lms by the motor is $(\mathcal{L} \qquad \mathcal{L}_i \ ) \ \mathcal{L}_i \qquad V t \ \mathcal{L}_i$. However, owing to lm-to- lm surfactant transport, this imposed strain is in general different from the strain that develops on the lms themselves as given by equation (2.10).

An important observation is that equation (2.13) now takes the form of an inhomogeneous, linear, rst order differential equation, albeit with variable coef cients, and this is the basis upon which we can solve it. The fact that the equation still turns out to be linear despite large strains

being imposed on the lms, relies in turn upon the lm tension model in equation (2.5) and also the linear relation between meniscus velocity and deviation in lm tension. Solutions of the system as obtained by [1] assumed small imposed strains or equivalently $V\,t \quad \mathcal{L}_i$ so in effect approximated the variable coef cient model by a constant coef cient one, leading to solutions in terms of exponentials. However that approximation will not be employed here.

Even without that approximation, there is still a scenario in which a constant coef cient case is recovered. The motor is only actually switched up to some time t_m. After that, $\mathcal{L}$ is held xed at a value $\mathcal{L}_m \quad \mathcal{L}_i \quad V\,t_m$ whereas $\mathrm{d}\mathcal{L} \quad \mathrm{d}t$ vanishes: equation (2.13) then reverts to having constant coef cients. Thus the model involves an initial motor driving phase followed by a subsequent relaxation phase, and solutions for both of these phases are required. The way in which to obtain solutions is outlined next.

3. Obtaining solutions of the model

Details of how to solve the model are given in appendix B, so only a brief outline will be given here. Solutions of the model are more conveniently expressed in dimensionless form (see appendix B(a)). Speci cally we de ne dimensionless lm lengths $L \quad = \mathcal{L} \quad \mathcal{L}_i$, and also dimensionless measures of the amount of surfactant on the lms $L_0 = \mathcal{L}_0 \quad \mathcal{L}_i$, along with dimensionless times $\quad = U \;\; t \;\; \mathcal{L}_i$. The dimensionless compression or stretch velocity v is de ned as $v = V \;\; U$. As appendix A explains, typical values of U (a physicochemical parameter of the foam lms) are well within the range of velocities V that a typical motor could attain. Hence it is possible to contemplate $v \quad 1$ for a motor operating far below its maximum velocity, but also $v \quad 1$ for a motor operating closer to maximum velocity. Strains are of course already dimensionless. However it is important to remember that here denotes the actual strain developed on the lm elements themselves, accounting for lm-to- lm surfactant transport. As already mentioned (see section 2(c)), these strains differ from the strains imposed on the lms by the action of the motors, which turn out to be $V\,t \;\; \mathcal{L}_i$ or equivalently (in dimensionless variables) v . Indeed the actual strains only become the same as the imposed strains when lm-to- lm surfactant transport is neglected. In general however, during motor motion, actual strains turn out to be smaller in magnitude than the imposed ones.

From here onward we work in terms of dimensionless variables. With the above de nitions for these variables, solutions of the model can now be obtained (see appendix B(b)). The method for obtaining solutions relies on replacing the dimensionless time by a modi ed time T which depends on both and v: within appendix B(b), see equations (B.13) and (B.18) along with Figure B1 and Figure B2. These equations for T are reproduced below

$$T \quad = \quad \frac{1}{l} \log(1 \quad v \quad) \tag{3.1}$$

$$T^{+} \quad = \quad \frac{1}{\overset{+}{l}} \log(1 + v \quad ^{+}) \tag{3.2}$$

These equations involve a limiting strain $\quad _l$, which is the actual strain on the lms that would be realised in the limit of large T , corresponding to signi cant amounts of either compression or stretch being imposed, albeit in the stretching case not yet accounting for ux possibly becoming plastic. The values of $\quad _l$ (see equations (B.11) and (B.16)) depend on the velocity v, with smaller v leading to smaller magnitude limiting strain. These equations for $\quad _l$ are reproduced below

$$_l \quad = \quad v \;\; (1 + v) \tag{3.3}$$

$$\overset{+}{l} \quad = \quad v \;\; (1 \quad v) \tag{3.4}$$

In the compressed case, the value of $\quad _l$, turns out to be negative, so we often write $\quad _l$ to make its sign explicit. Meanwhile in the stretched case, the formula for $\overset{+}{l}$ becomes problematic as v approaches and eventually exceeds unity. Solutions of the model then need to take a slightly different form in that case: details are given in appendix C.

When written in terms of modi ed time T , it turns out that the variable coef cient differential equation (2.13) converts to a constant coef cient one, so even though imposed strains no longer need to be small, solutions just involve exponentials but in terms of T not : see equations (B.14) and (B.19). These equations for are reproduced below

$$= \quad _l \ (1 \quad \exp(\quad T \ )) \tag{3.5}$$

$$^+ \quad = \quad ^+_l (1 \quad \exp(\quad T^+)) \tag{3.6}$$

As has been mentioned already, in the compressed case, strains are negative. In the stretched case, strains are positive, but we can encounter circumstances in which $^+$ reaches the value of unity, at which point lm-to- lm surfactant transport becomes very plastic (as section 2(b)iii explained). This occurs at a modi ed time that we denote $T^+_{\rm pl}$ or equivalently at an imposed strain that we denote $v \ ^+_{\rm pl}$. Formulae for $T^+_{\rm pl}$ and $v \ ^+_{\rm pl}$ are easy to derive starting from (3.6) and also (3.2) (equivalently (B.19) and (B.18)). The relevant formulae are given in equations (B.21) and (B.22), and ultimately just depend on v. As one might expect, increasing v causes $^+$ to attain the value of unity sooner, as will be veri ed shortly.

The above mentioned approach de ning a modi ed time T is only needed as long as motors are driving the system. Motors are however stopped at some well-de ned time $_m$ or equivalently some well-de ned imposed strain $v \ _m$, corresponding to lm lengths L_m and instantaneous strains in the lms $_m$. The system is then allowed to relax by exchanging surfactant even though lm lengths are now held xed. A solution for directly in terms of is then available. Again exponential solutions occur: see equation (B.23) within appendix B(b)iii. This equation is also reproduced below

$$= \ _m \exp(\quad (\qquad _m) \ L_m) \tag{3.7}$$

Once is known via either equation (3.5), (3.6) or (3.7), it is simple to nd the amount of surfactant on lms L_0 , using the value of and also the lm length L . The equations needed are dimensionless analogues of (2.10) and (2.14): see equations (B.2)–(B.3) and (B.5)–(B.6).

This completes our brief outline of how solutions are obtained. Results showing how the various solutions behave are described next.

4. Results

This results section is divided up into three subsections. The rst of these presents results for the compressed lm case (section 4(a)), while the second presents the stretched lm case (section 4(b)). Finally systems are considered that are allowed to relax after being either compressed or stretched (section 4(c)).

(a) Compressed lm

In the compressed lm case, we present data rst for the strain on lm (section 4(a)i) and then for the resulting amount of surfactant on the lm (section 4(a)ii).

(i) Strain during compression

Data for compressive strains (or more precisely for relative to $_l$) are presented in Figure 2. Speci cally in Figure 2(a) we plot this against dimensionless time , although an indication of what this represents in terms of dimensional time is discussed in appendix D. Note that (see Figure B1(a) in appendix B) for a given time , increasing v, leads to an increased T , and hence a that (according to equation (3.5) or equivalently equation (B.14)) in relative terms is closer to the limiting strain $_l$. This then is what we see in Figure 2(a). The case that is in relative terms furthest away from from $_l$ for longest is the limiting case $v \quad 0$, corresponding to a very slow stretch. In this particular case takes quite some time to evolve from zero to $_l$. However in fact barely changes at all in absolute terms, because $_l$ is itself vanishingly small in the $v \quad 0$ limit.

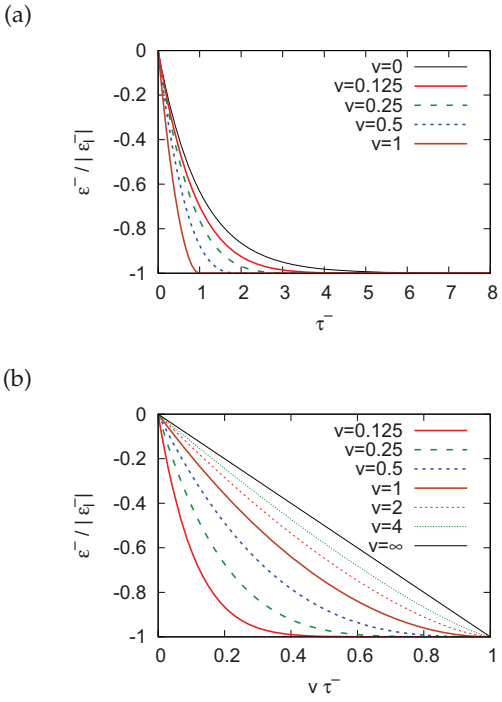

Figure 2. Compressed film: (a) $\varepsilon^-/|\varepsilon_l^-|$ versus τ^-, (b) $\varepsilon^-/|\varepsilon_l^-|$ versus $v\,\tau^-$.

Rather than plotting data against τ^-, it is also possible to plot against $v\,\tau^-$ (see Figure 2(b)). As has been mentioned, physically $v\,\tau^-$ represents an imposed strain, i.e. the length change imposed on the compressed film divided by its initial length. For a given $v\,\tau^-$ (i.e. a given imposed strain), increasing v leads to a smaller T^- (see Figure B1(b) in appendix B) and hence a ε^- that in relative terms is further away from $-|\varepsilon_l^-|$. That is what we see in Figure 2(b). Note however that Figure B1(b) also shows that for $v\,\tau^-$ close to unity (corresponding, according to equation (B.2), to a film compressed to a tiny fraction of its initial length), the value of T^- is always very large, regardless of the value of v. In that limit then (again according to equation (3.5) or equivalently equation (B.14)), ε^- always approaches $-|\varepsilon_l^-|$ for any v, which again is seen in Figure 2(b).

(ii) Surfactant on film during compression

In Figure 3 we show the evolution of $L_0^- \equiv L^-/(1+\varepsilon^-)$. This measures the amount of surfactant on the compressed film, or more specifically, in the dimensionless system considered here, it measures the amount of surfactant on the compressed film at any given instant relative to the amount that was on the film initially. Clearly the evolution of L_0^- is sensitive to the imposed velocity v: to evaluate it, equation (3.5) (equivalently equation (B.14)) is required along with equation (B.2). In all cases, the initial rate of change of L_0^- vanishes (which follows since ε^- vanishes initially, meaning there is no film tension difference to drive surfactant transport). However in cases with small v, we see L_0^- start to change significantly even after small imposed strains (i.e. even for relatively small $v\,\tau^-$) and after that L_0^- tends to follow the evolution of the film length L^-: indeed in the case $v \to 0$, the value of L_0^- always equals L^- for any specified imposed strain. On the other hand, for larger v, the value of L_0^- remains high even out to imposed strains $v\,\tau^-$ that are not so far from unity. However, even for these larger v values, in the limit as $v\,\tau^- \to 1$ (such that, according to equation (B.2), the compressed film length L^- becomes

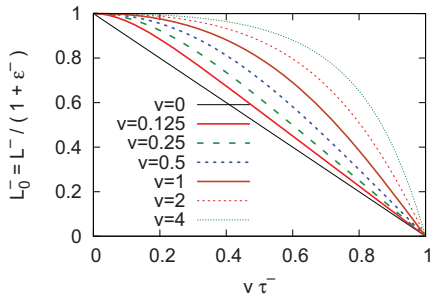

Figure 3. Compressed film: $L_0^- \equiv L^-/(1+\varepsilon^-)$ versus $v\,\tau^-$.

exceedingly small), we also see small L_0^- values, i.e. all surfactant can be eventually driven off the film, rather than simply accumulating on it.

(b) Stretched film

Now we turn to the stretched case, starting off by presenting data for the strain (section 4(b)i). Strains can however sometimes become large enough for the surfactant flux to become plastic, so conditions for this to occur are considered in section 4(b)ii. The amount of surfactant on the stretched film is analysed in section 4(b)iii.

(i) Strain during stretching

In the case of a film subjected to stretching, data for strain ε^+ are shown in Figure 4. Data in Figure 4(a) are plotted against dimensionless time τ^+, although appendix D indicates what this represents in dimensional time. For any fixed τ^+, it is found that increasing the value of v, decreases the value of T^+ (see Figure B2 in appendix B) and hence (according to equation (3.6) or equivalently equation (B.19)) moves ε^+ in relative terms further from the limiting strain ε_l^+, as seen in Figure 4(a).

As well as plotting against time τ^+, it is also possible (see Figure 4(b)) to plot data against imposed strain $v\,\tau^+$, which physically is the change in stretched film length divided by its initial length. In fact, at fixed $v\,\tau^+$ (i.e. fixed imposed strain), increasing v also tends to decrease T^+ (as is evident from equation (3.2) along with equation (3.4), or equivalently equation (B.18) along with equation (B.16)). Hence based on equation (3.6) or equivalently equation (B.19), in relative terms, ε^+ decreases compared to the limiting strain ε_l^+. However ε_l^+ itself increases with v according to equation (3.4) or equivalently equation (B.16). Hence even though (due to the decreased T^+), ε^+ is further from ε_l^+ in relative terms, it still might increase in absolute terms as v increases, which is what we see in Figure 4(b) in the various cases with $v \leq 1/2$ say.

Indeed it is only for very small v, such that limiting strains ε_l^+ are likewise small, that film strains ε^+ are always small in absolute terms regardless of the strain imposed $v\,\tau^+$: the solutions of [1] would then apply. However those solutions cease to apply if v increases. In that case, note also that, even if $v\,\tau^+ \gg 1$, then the value of T^+ which according to equation (3.2) or equivalently equation (B.18) grows only logarithmically, need not be exceedingly large. Thus again ε^+ need not be exceedingly close to ε_l^+. This is particularly evident in Figure 4(b) in the case $v = 1/2$ which exhibits a slow approach to a limiting ε_l^+ value, which for this specific velocity turns out to be unity in line with predictions of equation (3.4) or equivalently equation (B.16). The slow fashion in which ε^+ approaches unity when $v = 1/2$ is captured by equation (B.20).

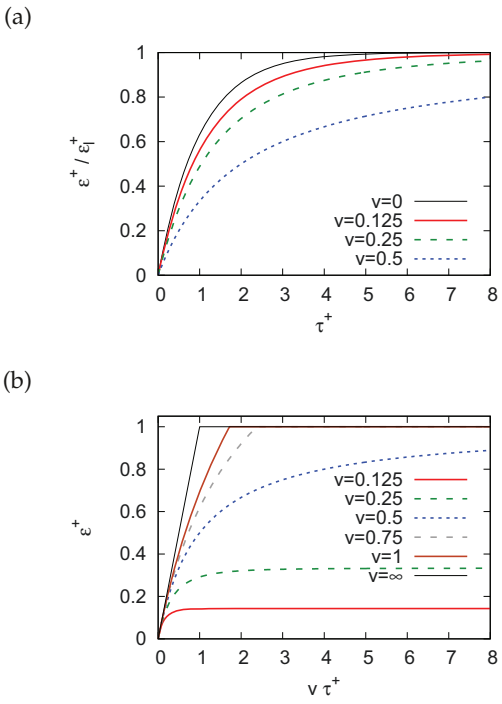

Figure 4. Stretched film: $\varepsilon^+/\varepsilon_l^+$ versus τ^+ (a) for stretching velocities $v \leq 1/2$ only, (b) ε^+ versus $v\,\tau^+$ including some larger v values.

Yet another feature of Figure 4(b) are the cases with $v > 1/2$. These are seen to reach $\varepsilon^+ = 1$ after some finite imposed strain, and surfactant transport then becomes plastic in order to keep ε^+ fixed at that value thereafter. This situation is discussed further in the next section.

(ii) Conditions for surfactant flux to become plastic

The imposed strain $v\,\tau_{\rm pl}^+$ required for the system to become plastic (as given by equation (B.22) or equation (C.7) depending on the v value) is plotted in Figure 5 as a function of v in the domain $v > 1/2$. Very large strains need to be imposed if v is only slightly greater than $1/2$, but as v increases, the value of $v\,\tau_{\rm pl}^+$ falls. The smallest possible value of $v\,\tau_{\rm pl}^+$ is unity and is reached only when $v \to \infty$. Having now identified which conditions do not allow the surfactant transport to become plastic, and which conditions do allow this, we can proceed to examine the surfactant content on stretched films.

(iii) Surfactant on film during extension

The value of $L_0^+ \equiv L^+/(1+\varepsilon^+)$ is a measure of the surfactant on the stretched film: specifically the dimensionless quantity L_0^+ is the amount of surfactant currently on the film relative to the amount on it initially. This is plotted in Figure 6 as a function of imposed strain $v\,\tau^+$ for various stretching velocities v. To evaluate this, equation (3.6) (equivalently equation (B.19)) is required along with equation (B.5). In all cases, in the limit of very small imposed strain, the initial rate of change of L_0^+ vanishes owing to lack of any initial tension difference (see also equation (B.9)). However moving towards larger imposed strains we start to see L_0^+ increasing.

There are however two generic behaviours. The first behaviour exhibited for $v < 1/2$ (seen clearly in the zoomed out view in Figure 6(a)) is that even after a fairly small imposed strain, L_0^+

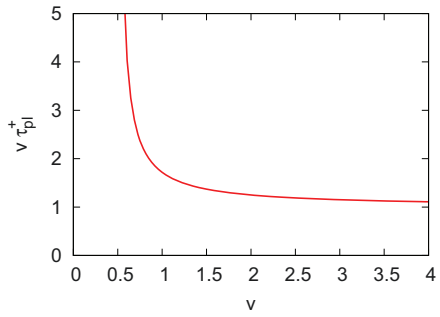

Figure 5. Imposed strain $v\,\tau^+_{\rm pl}$ versus v. Specifically, $v\,\tau^+_{\rm pl}$ is the strain that, when imposed on the stretched film, causes ε^+ to reach unity, and the surfactant flux onto the film then becomes plastic, transferring thereafter as much surfactant as is needed to keep ε^+ fixed.

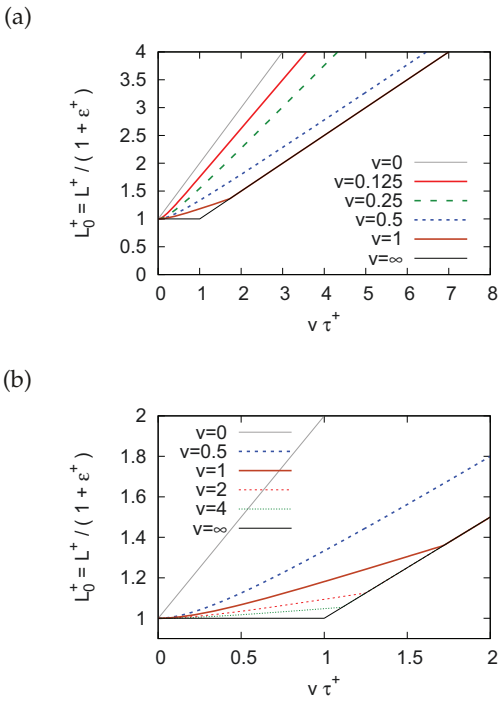

Figure 6. Stretched film: $L_0^+ \equiv L^+/(1+\varepsilon^+)$ versus $v\,\tau^+$. (a) Zoomed out view, (b) Zoomed in view, considering also some larger values for stretching velocity v.

asymptotes to a straight line behaviour. The value of L_0^+ does not grow quite as fast as that of L^+ but is close to it. Only for $v \to 0$ do we obtain $L_0^+ = L^+$. The second behaviour exhibited for $v > 1/2$ (seen clearly in the zoomed in view in Figure 6(b)) is that L_0^+ grows slowly with $v\,\tau^+$ at first, until eventually it is only half as large as L^+. We then see a sudden change in the rate of change of L_0^+, maintaining $L_0^+ = L^+/2$ thereafter. This condition is achieved sooner for larger v, but once it is achieved the value of L_0^+ depends on the imposed strain, but not on the individual

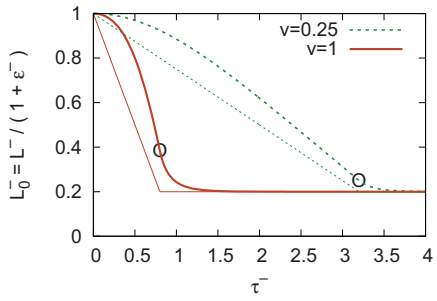

Figure 7. Compressed film: $L_0^- \equiv L^-/(1+\varepsilon^-)$ versus τ^- both during and after motor motion. The thinner straight lines indicate the corresponding values of L^-. The circled points represent the motor being switched off.

v. The case $v = 1/2$ is intermediate between these two aforementioned behaviours: it asymptotes to the line $L_0^+ = L^+/2$ but never actually reaches it.

(c) Incorporating both driving and relaxation phase

The results presented thus far concerned just the driving phase when the motor is switched on. In the present section, we consider both the driving phase and the subsequent relaxation phase. First we consider compression followed by relaxation (section 4(c)i) and after that stretch followed by relaxation (section 4(c)ii). Some additional discussion on how to compare the compression-relaxation and stretch-relaxation results can be found in appendix D.

(i) Compressing a film and then relaxing

In Figure 7 we show evolution of $L_0^- \equiv L^-/(1+\varepsilon^-)$ for a compressed film, with two different compression velocities, $v = 0.25$ and $v = 1$. In the figure, these L_0^- values (which measure the amount of surfactant on the film) are contrasted with L^- (measuring instantaneous film length). To evaluate L_0^-, equation (3.5) (equivalently equation (B.14)) and equation (B.2) are required. For both v values the motor is switched off when the film is compressed to 0.2 times its original length. Equation (3.7) or equivalently equation (B.23) now applies, whilst L^- is held fixed.

For both cases $v = 0.25$ and $v = 1$, initially the rate of change L_0^- is zero (as noted already in section 4(a)ii), but as the motor driving phase proceeds, the slope of the L_0^- curve shifts away from zero and (particularly in the case $v = 0.25$) tends towards a nearly constant slope. When the driving phase ceases, the higher velocity (i.e. $v = 1$) case has managed to retain more surfactant on the film than the $v = 0.25$ one does. In both cases however, L_0^- continues to decrease after the motor motion ceases, eventually relaxing back to the same final value as L^-. Moreover if we compare the time scale for the driving phase (e.g. the time scale for L_0^- to reach a constant slope) with the time scale for the relaxation phase, it is clear from Figure 7, that the relaxation time scale is shorter. This follows from equation (3.7) (equivalently equation (B.23)) when L_m^- (the final L^- value when the motor is switched off) is rather smaller than unity, corresponding to a rapid decay of ε^-, certainly more rapid than the evolution of ε^- during the motor driving phase.

(ii) Stretching a film and then relaxing

In Figure 8 we show $L_0^+ \equiv L^+/(1+\varepsilon^+)$ in a a stretched film case, with the film now being stretched to 5 times its original length, with the motor then being switched off. The velocities considered $v = 0.25$ and $v = 1$ are the same as those in Figure 7.

We consider the $v = 0.25$ case first. Equation (3.6) (equivalently equation (B.19)) and equation (B.5) apply up to the point that the motor is switched off. After motor switch off,

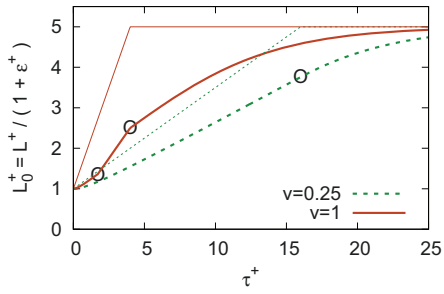

Figure 8. Stretched film: $L_0^+ \equiv L^+/(1+\varepsilon^+)$ versus τ^+ both during and after motor motion. The thinner straight lines indicate the corresponding values of L^+. In the case $v = 0.25$, the circled point represents the motor being switched off. In the case $v = 1$, the lower circled point represents the surfactant flux becoming plastic, and the upper circled point represents the motor being switched off.

equation (3.7) or equivalently equation (B.23) applies instead, with L^+ now held fixed. As already noted in section 4(b)iii, at initial time, the rate of change of L_0^+ is zero, but L_0^+ soon evolves (after some characteristic time scale) towards growing at a nearly constant rate. After the motor is switched off, L_0^+ continues to grow albeit by fairly modest amounts, relaxing towards L_m^+ (which is the value of film length L^+ when the motor is switched off). However the relaxation time scale is now longer than the characteristic time scale during the motor driving phase. This is in line with the predictions of equation (3.7) or equivalently equation (B.23) which suggest that the relaxation time in this dimensionless system itself scales like L_m^+ a quantity which is now rather larger than unity, hence implying slow relaxation.

The case $v = 1$ is a little different. During the motor driving phase, the value of L_0^+ does not grow nearly as fast as that of L^+. Equation (3.6) (equivalently (B.19)) and equation (B.5) still apply during this stage, although for $v = 1$, equation (3.6) simplifies to equation (C.8). However this situation soon ceases to apply. Instead we see a sudden increase in the rate of change of L_0^+ at the instant when L_0^+ becomes only half of L^+. However this increase in the rate of change of L_0^+ is undone when the motor motion stops, and the relaxation phase begins. In that case, as has been mentioned equation (3.7) or equivalently equation (B.23) now applies with L^+ held fixed, and this predicts ε^+ falling. Hence not only does $L_0^+ \equiv L^+/(1+\varepsilon^+)$ rise, but the ratio $L_0^+/L^+ = 1/(1+\varepsilon^+)$, which was formerly equal to one half, must rise also.

We then see quite a long time scale relaxation, after which L_0^+ eventually reaches the same value as L^+ (i.e. it reaches the value L_m^+). When $v = 1$, the amount of increase in L_0^+ during the relaxation phase is very significant (i.e. very significant amounts of surfactant transport occur even during this phase, which follows from equation (B.6) with L^+ fixed but ε^+ decaying all the way from unity to zero during the relaxation phase). Indeed when $v = 1$ more surfactant is transported during the relaxation phase than during the motor driving phase.

A final comment we make is that both Figure 7 and Figure 8 are plotted in terms of dimensionless time. These figures indicate that various different dimensionless time scales are involved during compression, relaxation after compression, stretch and relaxation after stretch. What the various time scales correspond to in dimensional variables is discussed in appendix D.

This now completes our analysis of the model of [1] considering the general case in which the compression imposed or stretch imposed upon films is significant. To summarise, the model admits very different behaviours between low imposed velocity and high imposed velocity, between compression and stretching, and between motor driving and relaxation phases. Overall conclusions are discussed in the next section.

5. Conclusions

We have considered a model (originally proposed by [1]) for how surfactant is transported from lm to lm around a meniscus within a foam. The key idea of the model is that there is a relation (in effect a constitutive relation) between lm-to- lm surfactant transport rate and tension differences between adjacent lms. Tension differences are in turn related to lm strains using a Gibbs elasticity parameter. Although the Gibbs elasticity could in principle depend on strain, it is treated here as constant which leads to a simple analytically tractable model.

The model has been applied to describe surfactant transport in a ve- lm device (two compressed lms on one side, two stretched lms on the other, plus a central lm joining them). The model makes a distinction between the strain imposed on the lms by a motor that drives them and the actual strain developed on the lm elements themselves. By assumption the central lm is not strained, but strains certainly develop in the compressed and stretched lms. The work of [1] restricted consideration, at least as far as solutions for the ve- lm device as a whole were concerned, to situations in which the strain imposed on either the compressed or stretched lms and consequently also the actual strain developed on the lm elements is small. This was done despite the fact that the constitutive model employed could actually cope with large strains. Indeed if the imposed strain is large enough and if it is also imposed rapidly enough, strain on the lm elements need not be small. This then is the case considered in the present work. Despite the fact that strains can now be rather large, the model remains analytically tractable, albeit solutions become more complicated than those presented by [1].

Knowing the instantaneous length of each lm, and the instantaneous strain on the lm elements within it, gives a measure of the instantaneous amount of surfactant contained on each lm, and thereby also, the amount of surfactant that has been transported off the compressed lm and/or onto the stretched one. In particular in the case of the compressed lm, even if it is compressed down to just a tiny fraction of its original length, the strain within the lm itself remains limited at a value set by the compression velocity. The larger the compression velocity, the larger magnitude of the limiting compressive strain. This then determines the amount of surfactant retained by the compressed lm, but much of the surfactant originally in place has simply been transported off it.

The case of the stretched lm is somewhat different. If the lm is stretched slowly enough, the strain on it reaches (as in the compressed case) a limiting value that depends on velocity. This limiting value can be approached if the stretch that is imposed is large, but only if the velocity of stretching is not too large. On the other hand, if the lm is stretched fast enough for long enough, it reaches a certain strain at which the behaviour suddenly changes. Surfactant ux jumps to a larger value than before to prevent the lm strain (and the lm tension that depends upon it) from growing any further. The reason that strain cannot grow further is associated with so called geometrical frustration: locally near the meniscus, different sides of a lm behave differently, and in particular strong stretching leads to very strong surfactant depletion, but only on one side of the lm. The strain we see moving slightly away from the meniscus is however not quite so large, as the two sides adjust towards an average strain value. The lm strain only begins to relax after the imposed stretching is stopped. However signi cant surfactant mass transfer onto the lm continues even as relaxation of the strain proceeds.

Although the model predicts interesting behaviour, it is worth re ecting that, as formulated here, it has only been studied for a ve- lm device, not for a more general foam. Nonetheless the compression and stretching processes that occur in the ve- lm device do capture some of the processes that also occur in a general foam. Speci cally the topological transformations (mentioned in the introduction) that occur very generally in foams involve certain lms being compressed and shrinking down until they vanish, whilst newly created lms are strongly stretched after they are formed. Moreover as a newly created lm stretches, any lms that neighbour it must shrink to compensate. What is clear is that these topological transformation processes do impose large strains on lms participating in them. In that respect, the fact that the

present work has managed to obtain model solutions involving large imposed strains seems to be particularly signi cant.

As formulated though, one of the issues with the model is that it is a lumped parameter model, which allows strains (and lm tensions that depend on them) to vary from lm to lm but not along individual lms. Thus the rate determining step for surfactant transport is in effect assumed to be transport around the meniscus, rather than transport along the lms themselves. The relation proposed between surfactant ux at the meniscus and lm-to- lm tension difference should apply to a general foam (indeed there is no reason to suppose it applies only for the ve- lm device). However, a challenge is to know whether the tension difference can always be treated as a lumped parameter for an entire lm, or whether instead some more local measure of tension difference must be used. Addressing questions like this can then help to elucidate the role that surfactant physical chemistry will have in determining foam rheology.

Ethics. This research raises no ethical issues.

Data Accessibility. This study has no data. All results presented here are obtained from formulae provided in the appendices in supplementary material.

Authors Contributions. This is a single author paper: the author conceived the study, carried out the necessary analysis, generated the results and drafted the paper. The author approved the nal version and agrees to be accountable for all aspects of the work.

Competing Interests. The author declares no competing interests.

Funding. The author acknowledges support from EPSRC grant EP/V002937/1.

References

1. Bussonnière A, Cantat I. 2021 Local origin of the visco-elasticity of a millimetric elementary foam. *J. Fluid Mech.* **922**, A25. doi: 10.1017/jfm.2021.529.
2. Vignès-Adler M. 2013 The zzling foam of champagne. *Angew. Chem. Int. Ed.* **52**, 187–190. doi: 10.1002/anie.201207299.
3. Durian DJ, Raghavan SR. 2010 Making a frothy shampoo or beer. *Phys. Today* **May**, 62–63. doi: 10.1063/1.3431341.
4. Völp AR, Kagerbauer L, Engmann J, Gunes DZ, Gehin-Delval C, Willenbacher N. 2021 In-situ rheological and structural characterization of milk foams in a commercial foaming device. *J. Food Eng.* **290**, 110150. doi: 10.1016/j.jfoodeng.2020.110150.
5. Ran L, Jones SA, Embley B, Tong MM, Garrett PR, Cox SJ, Grassia P, Neethling SJ. 2011 Characterisation, modi cation and mathematical modelling of sudsing. *Colloids and Surf. A, Physicochem. and Engg Aspects* **382**, 50–57. doi: 10.1016/j.colsurfa.2010.11.028.
6. Stevenson P, editor. 2012 *Foam engineering: Fundamentals and applications*. Chichester, UK: John Wiley and Sons.
7. Jameson GJ, Fuerstenau MC, Yoon RH, editors. 2007 *Froth flotation: A century of innovation*. Littleton, CO: Society for Mining, Metallurgy and Exploration.
8. Lemlich R, editor. 1972 *Adsorptive bubble separation techniques*. New York, London: Academic Press Inc.
9. Shan D, Rossen WR. 2004 Optimal injection strategies for foam IOR. *SPE J.* **9**, 132–150. doi: 10.2118/88811-PA.
10. Grassia P, Mas-Hernández E, Shokri N, Cox SJ, Mishuris G, Rossen WR. 2014 Analysis of a model for foam improved oil recovery. *J. Fluid Mech.* **751**, 346–405. doi: 10.1017/jfm.2014.287.
11. Wang S, Mulligan CN. 2004 An evaluation of surfactant foam technology in remediation of contaminated soil. *Chemosphere* **57**, 1079–1089. doi: 10.1016/j.chemosphere.2004.08.019.
12. Meghdadi A, Jones SA, Patel VA, Lewis AL, Millar TM, Carugo D. 2021 Foam-in-vein: A review of rheological properties and characterization methods for optimization of sclerosing foams. *J. Biomed. Mater. Res. B, Appl. Biomater.* **109**, 69–91.
13. Weaire D, Hutzler S. 1999 *The physics of foams*. Oxford: Clarendon Press.
14. Cantat I, Cohen-Addad S, Elias F, Graner F, Höhler R, Pitois O, Rouyer F, Saint-Jalmes A. 2013 *Foams: Structure and dynamics*. Oxford, UK: OUP.
15. Thomson W. 1887 LXIII. On the division of space with minimum partitional area. *Phil. Mag.* **24**, 503–514. doi: 10.1080/14786448708628135.

16. Weaire D, Phelan R. 1994 A counter-example to Kelvin s conjecture on minimal surfaces. *Phil. Mag. Lett.* **69**, 107–110. doi: 10.1080/09500839408241577.
17. Kraynik AM, Reinelt DA, van Swol F. 2003 Structure of random monodisperse foam. *Phys. Rev. E* **67**, 031403. doi: 10.1103/PhysRevE.67.031403.
18. Kraynik AM, Reinelt DA, van Swol F. 2004 Structure of random foam. *Phys. Rev. Lett.* **93**, 208301. doi: 10.1103/PhysRevLett.93.208301.
19. Höhler R, Cohen-Addad S. 2005 Rheology of liquid foam. *J. Phys.: Condens. Matter* **17**, R1041–R1069. doi: 10.1088/0953-8984/17/41/R01.
20. Princen HM. 1983 Rheology of foams and highly concentrated emulsions: I. Elastic properties and yield stress of a cylindrical model system. *J. Colloid Interface Sci.* **91**, 160–175.
21. Kraynik AM. 1988 Foam ows. *Ann. Rev. Fluid Mech.* **20**, 325–357.
22. Reinelt DA, Kraynik AM. 1996 Simple shearing ow of a dry Kelvin soap foam. *J. Fluid Mech.* **311**, 327–342. doi: 10.1017/S0022112096002613.
23. Reinelt DA, Kraynik AM. 2000 Simple shearing ow of dry soap lms with tetrahedrally close packed structure. *J. Rheol.* **44**, 453–471. doi: 10.1122/1.551096.
24. Evans ME, Kraynik AM, Reinelt DA, Mecke K, Schroder-Turk GE. 2013 Networklike propagation of cell-level stress in sheared random foams. *Phys. Rev. Lett.* **111**, 138301. doi: 10.1103/PhysRevLett.111.138301.
25. Biance AL, Cohen-Addad S, Hohler R. 2009 Topological transition dynamics in a strained bubble cluster. *Soft Matter* **5**, 4672–4679. doi: 10.1039/B910150K.
26. Torres-Ulloa C, Grassia P. 2022 Viscous froth model applied to the motion and topological transformations of two-dimensional bubbles in a channel: Three-bubble case. *Proc. Roy. Soc. London Ser. A* **478**, 20210642. doi: 10.1098/rspa.2021.0642.
27. Golemanov K, Denkov ND, Tcholakova S, Vethamuthu M, Lips A. 2008 Surfactant mixtures for control of bubble surface mobility in foam studies. *Langmuir* **24**, 9956–9961. doi: 10.1021/la8015386.
28. Couder Y, Chomaz JM, Rabaud M. 1989 On the hydrodynamics of soap lms. *Physica D* **37**, 384–405. doi: 10.1016/0167-2789(89)90144-9.
29. Edwards DA, Brenner H, Wasan DT. 1991 *Interfacial transport processes and rheology*. Boston: Butterworth-Heinemann.
30. Cohen-Addad S, Höhler R, Pitois O. 2013 Flow in foams and owing foams. *Ann. Rev. Fluid Mech.* **45**, 241–267. doi: 10.1146/annurev- uid-011212-140634.
31. Besson S, Debrégeas G. 2007 Statics and dynamics of adhesion between two soap bubbles. *Eur. Phys. J. E* **24**, 109–117. doi: 10.1140/epje/i2007-10219-y.
32. Besson S, Debrégeas G, Cohen-Addad S, Höhler R. 2008 Dissipation in a sheared foam: From bubble adhesion to foam rheology. *Phys. Rev. Lett.* **101**, 214504. doi: 10.1103/PhysRevLett.101.214504.
33. Denkov ND, Tcholakova S, Golemanov K, Ananthpadmanabhan KP, Lips A. 2009 The role of surfactant type and bubble surface mobility in foam rheology. *Soft Matter* **5**, 3389–3408. doi: 10.1039/B903586A.
34. Cantat I. 2013 Liquid meniscus friction on a wet plate: Bubbles, lamellae and foams. *Phys. Fluids* **25**, 031303. doi: 10.1063/1.4793544.
35. Cohen-Addad S, Höhler R. 2014 Rheology of foams and highly concentrated emulsions. *Curr. Opin. Colloid Interface Sci.* **19**, 536–548. doi: 10.1016/j.cocis.2014.11.003.
36. Seiwert J, Monloubou M, Dollet B, Cantat I. 2013 Extension of a suspended soap lm: A homogeneous dilatation followed by new lm extraction. *Phys. Rev. Lett.* **111**, 094501. doi: 10.1103/PhysRevLett.111.094501.
37. Embley B, Grassia P. 2011 Viscous froth simulations with surfactant mass transfer and Marangoni effects: Deviations from Plateau s rules. *Colloids and Surf. A, Physicochem. and Engg Aspects* **382**, 8–17. doi: 10.1016/j.colsurfa.2011.01.013.
38. Vitasari D, Cox S, Grassia P, Rosario R. 2020 Effect of surfactant redistribution on the ow and stability of foam lms. *Proc. Roy. Soc. London Ser. A* **476**, 20190637. doi: 10.1098/rspa.2019.0637.
39. Kern N, Weaire D, Martin A, Hutzler S, Cox SJ. 2004 Two-dimensional viscous froth model for foam dynamics. *Phys. Rev. E* **70**, 041411. doi: 10.1103/PhysRevE.70.041411.
40. Drenckhan W, Cox SJ, Delaney G, Holste H, Weaire D, Kern N. 2005 Rheology of ordered foams: On the way to discrete micro uidics. *Colloids and Surf. A, Physicochem. and Engg Aspects* **263**, 52–64. doi: 10.1016/j.colsurfa.2005.01.005.
41. Green TE, Bramley A, Lue L, Grassia P. 2006 Viscous froth lens. *Phys. Rev. E* **74**, 051403. doi: 10.1103/PhysRevE.74.051403.

42. Cox SJ, Weaire D, Mishuris G. 2009 The viscous froth model: Steady states and the high-velocity limit. *Proc. Roy. Soc. London Ser. A* **465**, 2391–2405. doi: 10.1098/rspa.2009.0057.
43. Cantat I. 2011 Gibbs elasticity effect in foam shear ows: A non quasi-static 2D numerical simulation. *Soft Matter* **7**, 448–455. doi: 10.1039/c0sm00657b.
44. Grassia P, Embley B, Oguey C. 2012 A Princen hexagonal foam out of physicochemical equilibrium. *J. Rheol.* **56**, 501–526. doi: 10.1122/1.3687442.
45. Satomi R, Grassia P, Cox SJ, Mishuris G, Lue L. 2013 Diffusion of curvature on a sheared semi-in nite lm. *Proc. Roy. Soc. London Ser. A* **469**, 20130359. doi: 10.1098/rspa.2013.0359.
46. Buzza D, Lu CY, Cates ME. 1995 Linear shear rheology of incompressible foams. *J. Physique II* **5**, 37–52. doi: 10.1051/jp2:1995112.
47. Exerowa D, Kruglyakov PM. 1997 *Foam and foam films: Theory, experiment, application*. Amsterdam, New York: Elsevier.
48. Lucassen-Reynders EH, Lucassen J, Garrett PR, Giles D, Hollway F. 1975 Dynamic surface measurements as a tool to obtain equation-of-state data for soluble monolayers. *Adv. Chem. Series* **144**, 272–285. doi: 10.1021/ba-1975-0144.ch021.
49. Loglio G, Pandol ni P, Miller R, Makievski AV, Ravera F, Ferrari M, Liggieri L. 2001 Drop and bubble shape analysis as a tool for dilational rheological studies of interfacial layers. In Möbius D, Miller R, editors, *Novel methods to study interfacial layers* vol. 11 *Studies in interface science* pp. 439–483. Amsterdam, London: Elsevier.
50. Loglio G, Tesei U, Pandol ni P, Cini R. 1996 A software-driven apparatus designed for measuring geometrical and physical properties of a large bubble formed at a capillary tip. *Colloids and Surf. A, Physicochem. and Engg Aspects* **114**, 23–30.
51. Fainerman VB, Miller R. 2001 Thermodynamics of adsorption of surfactants at the uid interfaces. In Fainerman VB, Möbius D, Miller R, editors, *Surfactants chemistry, interfacial properties, applications* vol. 13 *Studies in interface science* pp. 99–188. Amsterdam, London: Elsevier. doi: 10.1016/S1383-7303(01)80063-6.
52. van den Tempel M, Lucassen J, Lucassen-Reynders EH. 1965 Application of surface thermodynamics to Gibbs elasticity. *J. Phys. Chem.* **69**, 1798–1804. doi: 10.1021/j100890a002.
53. Mysels KJ, Shinoda K, Frankel S. 1959 *Soap films: Study of their thinning and a bibliography*. New York: Pergamon.
54. Karakashev SI, Manev ED. 2015 Hydrodynamics of thin liquid lms: Retrospective and perspectives. *Adv. Colloid Interface Sci.* **222**, 398–412. doi: 10.1016/j.cis.2014.07.010.
55. Vitasari D, Grassia P, Martin PJ. 2013 Surfactant transport onto a foam lamella. *Chem. Engng Sci.* **102**, 405–423. doi: 10.1016/j.ces.2013.08.041.
56. Bussonnière A, Shabalina E, X. Ah-Thon, Le Fur M, Cantat I. 2020 Dynamical coupling between connected foam lms: Interface transfer across the menisci. *Phys. Rev. Lett.* **124**, 018001. doi: 10.1103/PhysRevLett.124.018001.
57. Durand M, Stone HA. 2006 Relaxation time of the topological $T1$ process in a two-dimensional foam. *Phys. Rev. Lett.* **97**, 226101. doi: 10.1103/PhysRevLett.97.226101.
58. Grassia P, Oguey C, Satomi R. 2012 Relaxation of the topological $T1$ process in a two-dimensional foam. *Eur. Phys. J. E* **35**, 64. doi: 10.1140/epje/i2012-12064-3.
59. Satomi R, Grassia P, Oguey C. 2013 Modelling relaxation following $T1$ transformations of foams incorporating surfactant mass transfer by the Marangoni effect. *Colloids and Surf. A, Physicochem. and Engg Aspects* **438**, 77–84.
60. Grassia P. 2021 Surfactant transport between foam lms. *J. Fluid Mech.* **928**, F1. doi: 10.1017/jfm.2021.690.